664531 68

DP-925

AEC RESEARCH AND DEVELOPMENT REPORT

HEAVY WATER MODERATED POWER REACTORS

PROGRESS REPORT
JULY-AUGUST 1964

Technical Division
Wilmington, Delaware

DU PONT
REG. U. S. PAT. OFF.

ISSUED BY

Savannah River Laboratory

Aiken, South Carolina

Printed in USA. Price $1.25
Available from the Clearinghouse for Federal Scientific
and Technical Information, National Bureau of Standards,
U. S. Department of Commerce, Springfield, Virginia

664531

DP-925

Reactor Technology
(TID-4500, 33rd Ed.)

HEAVY WATER MODERATED POWER REACTORS PROGRESS REPORT

July–August 1964

D. F. Babcock, Coordinator
Power Reactor Studies
Wilmington, Delaware

Compiled by R. R. Hood

Issue Date: September 1964

Issued by

E. I. DU PONT DE NEMOURS & COMPANY
SAVANNAH RIVER LABORATORY
AIKEN, SOUTH CAROLINA

CONTRACT AT(07-2)-1 WITH THE UNITED STATES ATOMIC ENERGY COMMISSION

ABSTRACT

The Heavy Water Components Test Reactor (HWCTR) was operated intermittently during July and August for fuel irradiation tests. Severe pitting attack of the carbon steel tubes of the steam generators resulted from temporary inadequate removal of oxygen from the feedwater to the generators. The feedwater control and treatment were modified to eliminate further rapid attack of the tubes.

Physics calculations indicate that the removal of a single fuel assembly from an operating D_2O-cooled reactor would cause flux peaks of less than 5% in adjacent fuel positions at lattice pitches of practical interest.

Fabrication was started on driver fuel assemblies of uranium oxide for the HWCTR.

Design parameters were formulated for use in design studies of a 1000-MWe D_2O-cooled-and-moderated reactor that could be operated in the 1970's. Kinetics studies of the 1000-MWe reactor indicate that the turbine and reactor systems can be controlled and protected by normal control design.

CONTENTS

LIST OF TABLES AND FIGURES

HEAVY WATER MODERATED POWER REACTORS
PROGRESS REPORT
July–August 1964

INTRODUCTION

This report reviews the progress of the Du Pont development program on heavy-water-moderated power reactors. The over-all goal of the program is to advance the technology of these reactors so that they could be used in large power stations to generate electricity at fully competitive costs. Program emphasis is being placed on reactors that are cooled by liquid D_2O. Most of the effort is concerned with (1) the irradiation of candidate fuels and other reactor components in the Heavy Water Components Test Reactor (HWCTR), and (2) the development of low-cost fuel tubes for use in large water-cooled reactors.

SUMMARY

The HWCTR was operated at 41 to 45 MW during July and August for fuel irradiation tests; two outages were incurred - one scheduled and one unscheduled. Severe pitting attack of the carbon steel tubes of the two steam generators was discovered during this period. The attack occurred on the secondary side of the tubes, was of recent origin, and was attributed to inadequate removal of oxygen from the feedwater. Modified feedwater control and treatment, including in-line oxygen analyses, have been instituted, and plans were formulated to replace the tube bundles early in 1965.

Two driver fuel tubes (Zr alloyed with 9 wt % ^{235}U) from the HWCTR were inspected for dimensional changes after irradiation to a maximum fission burnup of 0.79 atom %. The dimensional changes were modest, indicating that the drivers probably will be able to withstand exposure to the end of their reactivity lifetime (about 2% burnup).

Physics calculations indicate that the removal of a single fuel assembly from an operating D_2O-cooled reactor will cause flux peaks of less than 5% in adjacent fuel positions when the lattice pitch is near 10 inches (square). It does not appear that this effect is large enough to be an important drawback to on-power refueling of such a reactor.

Fabrication was started of the first set of 2-tube driver fuel assemblies of compacted uranium oxide for the HWCTR, and development was started on suitable procedures for welding spacing ribs to the fuel sheaths of later sets.

Design parameters were formulated for use in a design study of a 1000-MWe D_2O-cooled-and-moderated power reactor that could be built in the 1970's after demonstration of the main technical features in a prototype reactor. A conceptual design for the control system of the reactor was specified on the basis of calculations of reactivity worths of a variety of control configurations. Preliminary kinetics studies of the reactor indicate that the turbine and reactor system can be controlled and protected by normal control design.

DISCUSSION

I. THE HEAVY WATER COMPONENTS TEST REACTOR (HWCTR)

The HWCTR is a D_2O-cooled-and-moderated test reactor in which candidate fuel assemblies and other reactor components are being evaluated under conditions that are representative of large water-cooled D_2O-moderated power reactors. Currently, fuel assemblies of uranium oxide (mechanically compacted in Zircaloy sheaths) and assemblies of thorium metal (coextruded with Zircaloy cladding) are being irradiated in this reactor. Operating data are summarized in Tables I and II and in Figures 1 and 2. Irradiation tests currently in progress are summarized in Tables III and IV.

A. REACTOR OPERATION

The HWCTR was operated continuously at 41 MW for the first 13 days of July. On July 13, the reactor was shut down for investigation of abnormally high D_2O losses into the cooling water in No. 1 steam generator. Subsequent investigation (described below) revealed one leaking tube and general corrosion throughout the bundle on the cooling water side. After the steam generator was repaired, nuclear operation was resumed on July 26. The reactor operated at 43 to 45 MW until August 7, at which time the unit was shut down to begin a previously scheduled outage. The reactor was returned to service on August 26, and was operated at power for the remainder of the month.

B. STEAM GENERATOR CORROSION

Inspection of the two steam generators in July and August revealed much more severe pitting attack of the secondary side of the carbon steel tubes than would have been predicted from the results of the last previous inspection (in February 1964). Pit depths ranged as high as 85 mils. The accelerated corrosion was attributed to oxygen attack caused by a recent change in quality of the sodium sulfite that is used to scavenge oxygen from the feedwater. The sulfite residual in the generators always has been measured routinely as an indication of oxygen control, and an adequate excess of sulfite has been maintained consistently. However, the particular brand of catalyzed sulfite that had been employed since early 1964 reacts with dissolved oxygen too slowly to maintain the oxygen concentration in the generators at less than 0.05 ppm. To prevent a recurrence of the attack, modified feedwater treatment and controls, including continuous in-line analysis of feedwater for residual oxygen, have been instituted. The oxygen content of feedwater is now under good control at a suitably low value of 0.02-0.03 ppm. Possible major changes in feedwater treatment, including deaeration, also are being studied with the objective of eliminating both the corrosion problem and chronic slime formation in various heat exchangers.

It was concluded from inspection of the steam generators that the tubes may be nearing the end of their useful life, and it was recommended to the AEC that the generators be retubed as soon as possible; the goal is to accomplish the retubing by the time new driver fuel is installed in the HWCTR early in 1965.

The process (D_2O) side of the generators was in excellent condition.

C. FAILURE OF UO_2 ROD BUNDLE ASSEMBLY

Subsequent to the July 13 shutdown of the HWCTR, radioactivity in the system indicated that a fuel failure had occurred. The failure was traced to an assembly of Zircaloy-clad pelletized UO_2 rods that were being irradiated for the Canadians under the USAEC-AECL Cooperative Program. The assembly consisted of five 19-inch-long bundles, each containing 19 rods of 0.5-inch diameter. Prior to the failure, the assembly had reached a maximum exposure of 6500 MWD/MTU* at a maximum thermal rating ($\int k d\theta$) of about 30 watts/cm.

Following its uneventful removal from the reactor, the failed assembly was disassembled and inspected under water. The failed bundle was identified by activity release as the fourth from the top in the column of five bundles. A cursory examination revealed no visible evidence of distortion or damage to any of the bundles. However, two of the unfailed bundles were damaged during subsequent handling.

Cave examination of the failed bundle is scheduled to begin in September.

D. INSPECTION OF DRIVER FUEL TUBES

Two fuel tubes from the second set of HWCTR driver assemblies were inspected for dimensional changes after irradiation to a maximum fission burnup of 0.79 atom %.

* Megawatt-days per metric ton of uranium.

The two tubes were inspected previously at a maximum burnup of 0.34 atom % at a maximum core temperature of 540°C (DP-905 and DP-915). On the basis of the favorable results in the first inspection, the maximum core temperature was increased to 580°C to permit an increase in specific power in HWCTR irradiation tests. Because the effect of the higher temperature on the dimensional stability of the tubes was unknown, frequent interim examinations were scheduled to observe their behavior.

The results of the two inspections are compared in Table V. The dimensional changes were modest, indicating that continued operation of the drivers at 580°C will be feasible to at least about 1.2 atom % burnup, at which time the driver targets are scheduled to be replaced and another interim inspection will be made. The driver fuel probably will withstand exposure to its full reactivity lifetime (about 2% burnup).

E. LEAKAGE TEST OF CONTAINMENT BUILDING

During the August shutdown, the HWCTR containment structure was tested for leaks. The measured leakage at an internal pressure of 5 psig was 0.63% per day of the building volume. This leakage rate is essentially the same as that measured in a similar test a year ago (0.75%/day at 5 psig).

II. REACTOR PHYSICS

A. FLUX PEAKING DURING ON-POWER REFUELING

The removal of a single fuel assembly in an operating heavy water reactor generally will cause flux peaking in adjacent fuel positions. In addition, a localized power peak can be expected when a replacement fuel assembly not poisoned by fission products is inserted into the vacant lattice position. These perturbations are a potential disadvantage of on-power refueling. The following paragraphs describe calculations that were made to determine the magnitude of the first-named effect, i.e., flux peaking in adjacent fuel positions, over a range of possible lattice parameters. The calculations indicate that in practical D_2O-cooled reactors with square lattice pitches near 10 inches, the flux peaking will be less than 5%. This effect thus does not appear to be a major objection to on-power refueling, particularly if a flexible control system such as that described later in this report is used.

Since the effect considered in the calculations involves a single fuel assembly, the heterogeneous HERESY[1] code was used in preference to homogeneous multigroup methods. Most of the calculations were performed for a finite lattice of 69 fuel assemblies on a square pitch. This lattice was assumed to be infinite in the axial (vertical) direction and to be surrounded by an infinite sea of D_2O at 20°C. All fuel assemblies were of the same kind, and the calculations were performed first with the central fuel assembly present, and then with it absent. Absorptions in the outermost fuel assembly were assumed to be unaffected by the presence or absence of the central assembly, and were used for normalization purposes.

Lattice bucklings were fixed by the geometry, since the HERESY calculations implicitly assume criticality. These bucklings ranged from 120 to 200 μB*, depending on the pitch and thermal neutron absorption of the fuel assemblies. This is a fairly small variation, and can be assumed to be constant at 150 μB for the cases of most interest.

Thermal neutron absorption properties of a fuel assembly are characterized in the HERESY theory by a paramter δ. The relation between δ and the conventional cell properties (for $B_z^2 = 0$) is

$$\delta = \left(\frac{L^2}{DV}\right)\left(\frac{1-f}{f}\right) + \frac{1}{4\pi D}\left(\ell n \frac{L^2}{V} + 2.874\right) \qquad (1)$$

where L^2 and D are the diffusion area and diffusion coefficient for the moderator, f is the fraction of neutrons absorbed in the fuel assembly in a cell of arbitrary size, and V is the area of the cell in cm^2. Values of δ were chosen to cover a range of f of 0.96 to 0.99 at a 10-in. square pitch. The same value of δ at other pitches corresponds to the same fuel assembly, not to the same value of f. The values of L^2 and D in Equation (1) were 7491 cm^2 and 0.8315 cm, respectively.

Results are presented in Figure 3 as a function of square lattice pitch and of δ. Curve A, corresponding to an assembly f of 0.99 at a 10-in. square pitch, would be typical for a power reactor fuel assembly.

Two related calculations were made to determine the sensitivity of the results to buckling and moderator temperature. The effect of lowering the buckling to zero, as would be approximately the situation with on-power refueling, is shown as a single point in Figure 3 for pitch = 10 in. and f = 0.99. The increase in flux peaking over the corresponding point with $B_m^2 \approx 150$ μB is 2%. The increase due to heating the moderator to 80°C is less than 1%.

* One microbuck = 10^{-6} cm^{-2}

B. CONTROL SYSTEM FOR 1000-MWe D_2O POWER REACTOR

Many conceptual designs for D_2O power reactors include on-power refueling as a primary feature. One of the advantages of such refueling is the decrease in the amount of reactivity which must be held in the control rods after the reactor has reached its long-term steady state of operation. At this stage, the normal reactivity changes may be controlled by the refueling operation, and the control rods serve merely to trim the reactivity and to shape the flux distribution.

As part of the design study for a 1000-MWe D_2O-cooled power reactor (Section IV), physics calculations were made of the worth of various arrays of stainless steel control rods placed interstitially in a square fuel lattice of 10.5-in. pitch. These control systems are expected to be compatible with on-power refueling, provided that a chemical shim is used to control reactivity until the steady state is reached. Table VI is a summary of the control rods that were studied. Each is characterized by the HERESY parameter, δ, which was defined in Equation (1) of the previous section. These values of δ were computed in the P-3 approximation to transport theory. For each of the nine types of control rod, four different control arrays were considered, i.e., with the control rods placed at center-to-center distances equal to 2, 3, 4, and 5 fuel lattice pitches. Rod worths and absorption ratios between fuel and control were calculated by the HERESY code. Also, for a reference case, calculations were made of the worth of a single control rod placed in the center of the small fuel lattice shown in Figure 4. The calculations with the single control rod were used, after a correction for radial flux shape, to obtain the ratio of neutron absorptions in the control rod to neutron absorptions in a single fuel assembly. These absorption ratios were then translated into values of $\Delta k_{eff}/k_{eff}$ for the regular lattices of control rods simply by dividing by the desired ratio of fuel assemblies to control rods. The calculations for the fully controlled lattices yielded both absorption ratios and $\Delta k_{eff}/k_{eff}$ directly.

The results of the two types of Δk_{eff} calculations are shown in Figure 5. The agreement between the different methods is good. Absorption ratios from the single rod calculations are given in Figure 6. Two curves are plotted, corresponding to the ratios of absorptions between the control rods and the nearest and next-nearest fuel assemblies. Absorption ratios obtained from the calculations on the large lattices are shown in Figure 7. These ratios are corrected to a flat radial flux, and, as plotted, show the ratio of neutrons absorbed in one control rod to neutrons absorbed in a fuel assembly that is in the maximum flux.

In the more widely spaced control patterns, some flux peaking will occur in the fuel positions not immediately adjacent to a control rod. For example, when the pitch of the control array is three times the pitch of the fuel array (9:1 ratio of fuel assemblies to control rods), the fuel assemblies can be divided into three different groups with respect to their locations relative to the control system. With the heaviest control rods of Table VI ($1/\delta = 0.6887$), the relative neutron absorptions in the three different groups of fuel were calculated to be 1.0, 0.983, and 0.959; the lowest figure applies for the fuel adjacent to a control rod. This irregularity would be undesirable in an operating reactor.

Figures 5 through 7 were used as a basis for choosing a control system for the 1000-MWe reactor. Figure 8 illustrates the recommended lattice pattern for the reactor. Two overlapping control arrays were used, one array containing full-length rods for trim control, and the other array containing partial-length rods for vertical flux shaping. Each control rod array has a pitch equal to twice the fuel pitch. Thus, the over-all ratio of fuel assemblies to control rods within the controlled zone is 2:1. There are 76 full-length and 81 partial-length rods, all having the dimensions of Rod 5 (Table VI). The worth ($\Delta k_{eff}/k_{eff}$) of the rods to the controlled zone alone was calculated to be 6.1%. The worth to the full reactor would be about 5%, which satisfies the requirements on total k for the steady state loadings.

III. REACTOR MATERIALS

A. TUBES OF URANIUM OXIDE

1. Fabrication of Irradiation Test Specimens

As reported in DP-915, fabrication was completed on two fuel assemblies (SOT-8-2 and SOT-8-3), each comprising seven 13-in.-long UO_2 tubes 3.650 in. in outside diameter and containing UO_2 enriched to 1.2% ^{235}U. These Zircaloy-clad tubes resemble in cross section the largest fuel tube of the 3-tube reference design described in DP-830[2]. Both assemblies were charged into the HWCTR late in August; they are scheduled to operate at a reference design $\int k d\theta$ of 30 watts/cm to exposures as high as 30,000 MWD/MTU. Eight additional fuel tubes of this same design were completed and stored for possible future irradiation.

Eight tubes of the same nominal dimensions as the SOT-8 assemblies described above were loaded with UO_2 powder, vibratory compacted, and swaged; in contrast to the SOT-8 assemblies, these tubes contain UO_2 of slightly higher enrichment (1.7% ^{235}U) in order that higher thermal ratings (~40 watts/cm) can be achieved during irradiation tests. Current plans are to fit these tubes with chambered end plugs of the design being developed for UO_2 driver assemblies (Figure 9).

Fabrication of the thirty 2.55-in.-OD UO_2 tubes described in DP-915 was completed. These tubes simulate the intermediate tube of the 3-tube reference design and are available for irradiation at maximum thermal ratings of 30 and 40 watts/cm.

2. Oxide Driver Tubes for the HWCTR

Fabrication was started on a set of 2-tube driver fuel assemblies of mechanically compacted UO_2 for the HWCTR. These assemblies will be clad with Zircaloy-2 and will operate in the HWCTR at irradiation conditions of direct interest for D_2O-cooled power reactors. Each assembly will contain a 10-ft-long outer tube and a column of 3 shorter tubes positioned within the outer tube by means of ribbed washers. The dimensions of the tubes are listed in DP-915. Two sets of inner and outer tubes are to be fabricated by October for early evaluation and irradiation tests in the HWCTR. Twenty-four assemblies for a complete charge are scheduled to be completed by the end of 1964. The status of the oxide driver program is reviewed in the following paragraphs.

Raw Materials

Sheath tubing was received for twenty sets of inner tubes. Evaluation of the tubing is under way, and temporary end plugs are being fabricated. Approximately 340 pounds of 3.8% enriched UO_2 was received and is being crushed and sieved for vibratory compaction blends.

Mockup Fuel for Physics Tests

Twelve mockup fuel pieces of the 2-tube drivers were fabricated for preliminary physics measurements to determine flux and power distribution in the drivers as a function of ^{235}U loading. The twelve pieces have 14-inch-long cores of vibratory-compacted UO_2 in 0.030-inch-thick aluminum sheaths. Dimensions are as close to the OD and ID of the driver core as could be obtained with aluminum sheaths. The twelve pieces include two outer and two inner fuel sections of each of the following enrichments: 1.5, 3.0, and 4.5 wt % ^{235}U.

Prototype Elements for Fabrication Development

As described in DP-915, UO_2 loading studies were conducted on two prototype elements made with available tubing of slightly larger diameter but nearly the same wall thickness as the outer driver tube. A loading procedure was developed that will produce a satisfactory UO_2 density (82% of theoretical) in the vibratory compaction step. However, concentricity of inner and outer sheath tubing could not be improved over that previously attained (~0.015 in.); this results in a core thickness variation of ±9%, as compared with a previous standard specification of ±5% for UO_2 tubes. Calculations indicate that the larger variation can be tolerated in the drivers from a heat transfer standpoint; therefore, the wall thickness tolerance for the UO_2 drivers was relaxed to ±9%. The two prototype elements were swaged satisfactorily and will be fitted with end plugs of a new design (Figure 9) before undergoing further testing.

UO_2 Procurement

Delivery of fused and crushed UO_2 for the oxide drivers has been delayed because of unexpected difficulty by the vendor in reducing the nitrogen content to meet the specification of less than 50 ppm nitrogen by weight. Two outgassing treatments were tried by the vendor, namely:

a. Vacuum extraction at 1400°C for 4 hr

b. Hydrogen annealing at 1700°C for 4 hr

Neither method was entirely satisfactory. These results differ from earlier results (DP-845 and DP-865), in which hydrogen annealing and vacuum outgassing were effective in reducing nitrogen to very low levels. The reasons for this discrepancy are being investigated. Nevertheless, about 1800 pounds of fused UO_2 were treated and shipped. The nitrogen content was reduced from about 400-500 ppm to a range of 30 to 250 ppm. Only 30% of the oxide contained less than 50 ppm nitrogen; another 30% contained 50 to 100 ppm.

The larger nitrogen releases that could conceivably occur during irradiation will be accommodated by increasing the size of the void chambers at the ends of the fuel tubes. The short inner driver tubes, which present the more serious gas release problem, will be fabricated with UO_2 containing 100 ppm nitrogen or less. The long outer tubes, which can more easily afford space for large void chambers, will be loaded with UO_2 that contains 150 ppm nitrogen or less.

Chambered End Plug

In a new end plug design now being fabricated for test, the void chamber for collection of fission product gases is combined with the end plug. As shown in Figure 9, this new "chambered" end plug provides several improvements:

a. Inner and outer weld are in separate axial positions. Individual welds can then be made without overhang.

b. Extensive boring to remove oxide from the end of the fuel tube before inserting the void chamber is avoided. At the 2- to 3-inch depth required for the outer fuel tube, the boring operation would be very difficult and probably inaccurate.

c. If desired, short radial spacers can be welded directly on the new chambered end plug. Previously, it was not feasible to weld short spacers to the Zircaloy cladding.

3. Development of Welded Ribs for UO_2 Fuel Tubes

Following fabrication of the first set of UO_2 drivers, a similar set is planned with full-length Zircaloy ribs to space the fuel tubes. These drivers will consist of two nested tubes, each 10 ft long, with the 0.030-in. (possibly 0.060-in.) longitudinal spacer ribs attached by electron beam welding to either the inner sheath of the outer fuel tube or the outer sheath of the inner fuel tube. Development work is under way to compare these two alternative schemes.

Swaging Tests

In the first scheme, the rib will be welded to the inner sheath prior to fabrication of the fuel tube; the ribbed sheaths will then be loaded and swaged on a grooved mandrel. Five sheaths with short ribs attached by the electron beam process at Dresser Products, Inc., were received, assembled with outer sheaths, and are scheduled for preliminary swaging tests next month. The purpose of this initial test is to determine if ribbed-sheath fuel tubes can be swaged satisfactorily.

Electron Beam Welding

An electron beam welding facility was installed at Savannah River Laboratory, as described in DP-905. The welding facility is designed such that if swaging of tubes with internal ribs is not feasible, minor modifications to the equipment will allow ribs to be welded to the outside of finished, swaged tubes. This method is considered to be more difficult and to involve more risk to sheath integrity; therefore it will not be attempted unless internal ribs are shown to be impractical.

The welding facility comprises a commercial electron beam welder with 16-in.-diameter by 16-ft-long extensions attached to each side of the vacuum chamber, and a drive and positioning mechanism to position the ribs relative to the tube and to move the assembly accurately beneath the electron beam during welding. During this report period, nonuniform motion in the drive mechanism was corrected by replacing the lead screw and adding several bearing supports. Difficulties with several minor electronic components in the welder were corrected, and test welding of ribs in short sections of Zircaloy tubing was started.

Internal ribs will be welded to 30 Zircaloy housing tubes for the next HWCTR driver load beginning early in September, when the tubing is scheduled to be received. These housings, which have less stringent service requirements than sheath tubing, are the first to be welded. The operating experience will provide an opportunity to demonstrate the equipment and to refine techniques and weld parameters before progressing to the sheath tubing. Design and fabrication of a precision expanding mandrel to position four 0.060-inch-thick by 0.225-inch-high ribs within the 3.2-inch-ID Zircaloy housing tube have been completed. Finished dimensions of the mandrel and mechanical drive mechanism indicate that the tubes and ribs can be positioned with sufficient accuracy for the housing tube application.

A smaller expanding mandrel for positioning internal ribs on driver sheath tubing was designed. If the swaging tests described earlier demonstate the feasibility of fabricating internally ribbed tubes, this mandrel will be fabricated for welded ribs inside of full-length driver sheath tubing; techniques developed during housing tube welding will be adapted to the driver sheath tubing.

B. TUBES OF THORIUM METAL

Fabrication of two thorium-uranium alloy tubes was completed, and the tubes were charged into the HWCTR for an exploratory irradiation test. The objective of the test is to evaluate the performance of thorium tubes under irradiation conditions that would be encountered in operation of a liquid D_2O-cooled-and-moderated reactor operating on an equilibrium thorium-^{233}U fuel cycle. The tubes are 10 ft long, contain 1.5 wt % highly enriched uranium, and were coextruded with Zircaloy cladding. The nominal OD and wall thickness are 2.5 inches and 0.30 inch, respectively. The anticipated irradiation conditions are an exposure-averaged thorium temperature of 500°C (maximum) and exposures as high as 20,000 MWD/MT.

C. SURVEILLANCE OF HWCTR ZIRCALOY COMPONENTS

Irradiated Zircaloy components from the HWCTR are being examined to determine their present condition, changes in properties caused by irradiation, and the adequacy of similar components for continued use in the HWCTR (DP-915). Concern about the continued serviceability of these components resulted from failures of safety rod guide tubes and from subsequent observations that the corrosion and hydrogen content of the guide tubes were greater and the ductility lower than might be expected. Although this work was started because of HWCTR needs, the results should be of general interest wherever Zircaloy is used in nuclear reactors.

The first component to be examined in this program was a low-nickel Zircaloy-2 housing from one of the driver positions. The housing was irradiated in HWCTR from March 1962 until February 1964. Total operating time at tube temperatures of 180-210°C was approximately 6000 hours. The fast neutron (>1 Mev) exposure was 1.4×10^{20} nvt; the peak flux was estimated to be 4×10^{13} nv thermal and 6×10^{12} nv fast. The irradiation produced typical irradiation hardening; however, no evidence of inadequate ductility or tendency toward brittle behavior was observed in simple bend tests. Corrosion was substantially more severe than expected, but there was no danger from hydride embrittlement because the low-nickel Zircaloy-2 tubing absorbed very little of the hydrogen.

Based on the evaluation of this driver housing, the rest of the driver housings in HWCTR should exhibit adequate properties for continued operation throughout the present driver charge as presently scheduled. Future work on the housing will include hydrogen analyses and hydraulic burst tests to evaluate the mechanical properties.

In the postirradiation examination, estimates of the mechanical properties of the driver housing were made by bending full- and half-ring sections with a mechanical manipulator in a cave. The strength of the Zircaloy was measured by the force necessary to bend the sections, as indicated by a grip-force gage on the manipulator. The tendency of the Zircaloy toward low ductility or brittle behavior was estimated from the amount of deflection necessary to initiate cracks and failure.

Sections from the top of the tube exhibited strengths very similar to unirradiated sections. In the middle and lower sections of the tube, however, the strength was increased 50% by the neutron exposure. None of the sections cracked or failed even at full bend. Data for the half-ring sections are shown in Table VII.

The hydrogen content in the housing tube was estimated to be less than 50 ppm by metallography. Unirradiated samples contained about 10 ppm, which indicates that a pickup of 40 ppm or less occurred by in-pile corrosion. The hydride platelets were very small and appeared to be oriented predominantly parallel to the tubing surface, which is the most favorable orientation for minimum effect on transverse and longitudinal ductility.

The zirconium oxide films on the tube surfaces were mainly black, with a slight "milky" shade indicating the presence of post-transition oxide. The ZrO_2 thickness averaged 0.18 mil and ranged from 0.10 to 0.23 mil. The ZrO_2 thickness to be expected after the same time-temperature exposure out-of-pile is 0.03 mil. The film thicknesses correspond to weight gains of 67 mg/dm^2 in pile and 11 mg/dm^2 out of pile and to Zircaloy consumptions of 0.12 and 0.02 mil, respectively. The corrosion did not severely reduce the 30-mil wall thickness even though irradiation produced a sixfold increase in the corrosion rate. Irradiation effects similar to this have been observed at other laboratories.

The most interesting aspect of the corrosion data is the extremely small amount of hydrogen absorbed by the housings. Based on the metallographic estimates, the low-nickel Zircaloy-2 tubing absorbed less than 12% of the hydrogen theoretically released by corrosion. Similar analyses of the Zircaloy-2 safety-rod guide tubes indicated a hydrogen pickup of 50%. This comparison supports autoclave tests described by Westinghouse[3] in LiOH solutions in which Zircaloy-4 and low-nickel Zircaloy-2 exhibited hydrogen pickups that were 1/5 to 1/2 those for Zircaloy-2.

IV. REACTOR DESIGN AND EVALUATION STUDIES

In June 1964, the Du Pont Engineering Department was requested by the AEC to develop the design of a 1000-MWe D_2O-cooled-and-moderated power reactor in enough detail for a budget estimate of construction cost. This study is a direct continuation of two other design studies that have been completed: (1) a 300-MWe prototype reactor (DP-885), and (2) a feasibility study of D_2O reactors of large capacity (DP-915). The following paragraphs summarize information that has been developed to date for use in the study. The information is in two categories: (1) assumptions and design parameters, and (2) transient behavior of the reactor.

A. ASSUMPTIONS AND DESIGN PARAMETERS

The general guide lines and basic assumptions for the 1000-MWe reactor are as follows:

(1) A prototype reactor of about 300-MWe capacity will be critical by FY-1970. Experience gained through design, construction, and operation of the prototype reactor will be incorporated into the 1000-MWe design. Major features will be demonstrated in the 300-MWe installation or elsewhere before initial operation of the 1000-MWe plant.

(2) In addition to the construction of a prototype, a continuing research and development program will be carried out to improve the performance and economics of the plant.

(3) The plant design will be optimized for the economical production of electrical energy by use of nested fuel tubes of UO_2. No special provisions will be made in the design for operation with thorium fuel.

(4) The 1000-MWe plant will be rated for base load operation, but the design will include instrumentation, etc., required for load-following capability.

(5) The design and estimate will be based on a calandria concept with Zr - 2.5% Nb pressure tubes. However, a study will be made of internally insulated pressure tubes and of Zircaloy-2 or -4 as potential alternatives.

(6) The over-all estimate will be based on on-power refueling, but the differential cost between on-power and off-power schemes will be determined.

Basic design parameters for the 1000-MWe cost study are listed in Table VIII. The lattice arrangement, system flowsheet, and fuel cross section are shown in Figures 8, 10, and 11.

1. Steam Conditions

When the steam pressure for a given primary coolant temperature is optimized, the gain in thermal efficiency of a saturated steam cycle at high pressure is balanced against the increased cost of the heat transfer equipment. Where the fuel cycle cost is low, as in D_2O reactors, the optimum is reached at fairly low thermal efficiency and low capital cost. The optimum steam pressure is about 500 psi if the turbine cost is not influenced strongly by the throttle pressure. However, at a power of 1000 MWe, the throttle pressure has a strong influence. Because of size limitations on last stage blades, and the associated exhaust loadings, a single turbine-generator unit can be specified for 1000 MWe only if the throttle pressure is at least 600 psi. At lower pressures, two 500-MWe units must be provided at a significant increase in capital cost. For this reason, a throttle pressure of 600 was specified. Also, economizers were recommended as a means of increasing the temperature approach in the steam generators and thereby decreasing the required heat transfer area.

2. Heat Removal

The flowsheet shown in Figure 10, with economizers after the fourth feedwater heater, was predicted to be the optimum arrangement for the 1000-MWe reactor. Adding a fifth heater to raise the feedwater temperature to 207°C increases the thermal efficiency from 30.4 to 30.7%, but results in significantly lower temperature differences and higher heat transfer areas in the steam generators and economizers.

The power input to the heat exchangers is 3570 MW, of which 50 MW is pump power and 3520 MW is transferred to the coolant in the fuel assemblies. The total flow is 350,000 gpm of D_2O at 264°C, and the temperature rise in the reactor is 36°C.

3. Core Performance

The reactor core consists of 516 fuel assemblies, arranged as shown in Figure 8. Assemblies in Zones 2, 3, and 4 (the outer 3 rows of fuel assemblies) are expected to operate at 90%, 75%, and 60%, respectively, of the average flat zone assembly power, which is 7.6 MW. The ratio of maximum power to average power in the flat zone is maintained at about 1.2 in the axial direction by manipulation of partial-length control rods. This ratio is 1.4 in the buckled zone.

A 10.5-in. lattice pitch was specified by the Engineering Department as the minimum that would provide necessary clearances between the stacks of inlet and outlet piping and the shield tube extensions.

4. <u>Fuel Performance</u>

The fuel assembly concept proposed for the reactor is shown in cross section in Figure 11. It consists of three concentric tubes of mechanically compacted UO_2 in Zircaloy sheaths. These fuel tubes are separated from the pressure tube by a housing tube that can support the entire fuel assembly and can be removed from the reactor if necessary in the event of a fuel failure. Fuel tubes are spaced by means of ribs that are electron beam welded to the inner sheaths prior to loading the UO_2. The feasibility of this spacing concept has not been established (see Section IIIA).

Fuel assemblies are designed so that each coolant channel has the same coolant temperature rise and each fuel tube has the same minimum safety factor on heat transfer burnout. The fuel assembly has a minimum core thickness of 0.195 inch and a minimum coolant channel thickness of 0.180 inch. The maximum $\int kd\theta$ at 7.6 MW is 32 watts/cm (intermediate tube), and the maximum coolant velocity is 50 ft/sec (axial channel). The average exposure of the fuel is 20,000 MWD/MTU, and the $\int kd\theta$ of the hottest tube averaged over the exposure is about 35 watts/cm.

It is estimated that the power of a freshly charged assembly will be about 30% higher than the average, or 9.9 MW. The maximum $\int kd\theta$ at 9.9 MW is 42 watts/cm, and the maximum heat flux is 520,000 pcu/(hr)(ft^2) at the inner surface of the inner tube. If the flow-zoning efficiency is 90%, the coolant temperature rise in the hottest assembly is 51°C, and the resulting boiling margin at the outlet is 6°C. A steam quality of about 2% is expected at the outlet of the hottest subchannel.

Individual fuel positions are monitored for coolant flow, temperature rise, and activity. Flow and temperature monitoring are essential in this type of reactor to obtain the desired power at reasonable fuel temperatures and heat fluxes. The activity monitor provides the most sensitive indication of a fuel element failure.

B. TRANSIENT RESPONSE STUDIES

A preliminary study was initiated of the transient response of the 1000-MWe reactor system in order to assist in the design of the over-all plant control system, the design of the secondary steam system, specification of the safety relief system, and the requirements of the primary pressurizing system. The procedure and results are discussed below.

1. Reactor Model

The mathematical model used to simulate the plant is shown in Figure 12, in which the plant is subdivided into heat capacity blocks and instantaneous mixing of the coolant within each block is assumed. This approach has been used successfully in studies of the transient behavior of the Savannah River production reactors and of the HWCTR (DP-245). The equations expressing the enthalpy balance of the primary system are listed below:

$$H_1\dot{T}_1 = PP_o - U_1(T_1 - \overline{T})$$

$$2\overline{T} = T_2 + T_5$$

$$H_2\dot{T}_2 = U_1(T_1 - \overline{T}) - F_1(T_2 - T_5)$$

$$H_3\dot{T}_3 = F_1(T_2 - T_3)$$

$$H_4\dot{T}_4 = F_1(T_3 - T_4) - U_2(T_4 - T_8)$$

$$H_5\dot{T}_5 = F_1(T_4 - T_5)$$

where

H_1 = heat capacity of the fuel, MW-sec/^oC

$\dot{T}_1, \dot{T}_2, \dot{T}_3$, etc. = time derivatives of temperature, ^oC/sec

P = power of the reactor relative to the initial power

P_o = initial power of the reactor, MW

T_1 = effective temperature of the fuel, ^oC

$\overline{T}$ = average temperature of the coolant in the reactor core, ^oC

U_1 = product of the heat transfer coefficient and the heat transfer area of the fuel, $MW/^{o}C$

H_2 = heat capacity of the reactor coolant core, $MW\text{-}sec/^{o}C$

T_2 = outlet temperature of the reactor coolant, ^{o}C

T_5 = inlet temperature of the reactor coolant, ^{o}C

H_3 = heat capacity of the reactor coolant system from the reactor to the steam generator, $MW\text{-}sec/^{o}C$

T_3 = coolant temperature at the inlet to the steam generator, ^{o}C

H_4 = heat capacity of the steam generator including the fluid on the secondary side, $MW\text{-}sec/^{o}C$

T_4 = temperature of the D_2O leaving the steam generator, ^{o}C

F_1 = flow rate of the primary coolant, $MW\text{-}sec/^{o}C$

U_2 = product of the effective heat transfer coefficient and the heat transfer area in the steam generator, $MW/^{o}C$

H_5 = heat capacity of the primary coolant system from the steam generator to the inlet of the reactor, $MW\text{-}sec/^{o}C$

T_5 = inlet temperature to the reactor, ^{o}C

The equations that were used to described the secondary system are:

$$\dot{n}_s = G_s - G_1 \frac{(f_1 + f_2)}{m}$$

$$G_s mh = U_2(T_4 - T_6) - F_2(T_6 - T_8)$$

$$P_s = \frac{n_s R(T_6 + 273)}{V_s}$$

$$T_6 = f(P_s) \text{ for saturated steam}$$

where

n_s = the quantity of steam in the steam generator and piping, mols

G_s = the rate of formation of steam in the steam generator, mols/sec

G_1 = steam flow rate to the turbine, lb/sec

f_1 = relative flow rate to the turbine

f_2 = relative flow rate through the turbine bypass

m = pounds of steam per mol

h = heat of vaporization, MW-sec/lb

T_8 = temperature of the feedwater returning to the steam generator (assumed constant), ^oC

P_s = pressure of the steam in the steam generator, psia

V_s = combined volume of the steam in the steam generator and turbine piping, ft^3

R = gas constant, psi-$ft^3/^oK$ - mol

T_6 = temperature of the saturated steam, ^oC

The above equations were combined with the neutronic equations that are listed below:

$$\dot{C}_i = \lambda_i(P - C_i) \qquad i = 1, 2, 3, 4$$

$$P = \frac{\sum_1^4 \beta_i C_i}{\sum_1^4 \beta_i - k}$$

$$k = \alpha_1(T_1 - T_1^o) + \alpha_2(\overline{T} - \overline{T}^o) + k_1$$

where

C_i = concentration of the i^{th} precursor

λ_i = decay constant for the i^{th} group, sec^{-1}

β_i = yield of the i^{th} precursor group

k = excess reactivity

α_1 = temperature coefficient of the fuel, per ^oC

α_2 = temperature coefficient of the coolant, per °C

k_1 = change in reactivity caused by movement of the control and safety rods

The system is excited by one of the three driving functions listed below:

$$k_1 = k_1(t)$$

$$f_1 = f_1(t)$$

$$f_2 = f_2(t)$$

The values that were used for the input constants and steady-state conditions are shown in Table IX. These values closely approximate those associated with the design parameters in Table VIII.

2. Results

The nuclear behavior of the reactor system is relatively independent of changes in the turbine load since the coolant coefficient of reactivity is very close to zero. Thus, the behavior of the reactor system depends almost exclusively upon the reactor control system and the characteristics of the reactor core. To guide the control engineer in defining the control system required for matching the reactor power to the turbine load, calculations were made of the effects of load changes and upsets. The results indicate that the turbine and reactor systems can be controlled and protected by normal control design.

In the examples discussed below, load changes were simulated by step and ramp changes in the steam flow to the turbine. Also, the effects of a turbine trip followed by a reactor scram were studied as a function of the fraction of steam that is bypassed following the turbine trip-out.

Figure 13 shows the transient response following a step decrease of 5% in the steam flow to the turbine. Two cases are shown: in one there is no movement of the reactor control rods, and in the other the rods are moved for 30 seconds at a rate equivalent to -1.2×10^{-5} k/sec. With this movement of the control rods, the pressure of the steam increases from 500 to 515 psi in about 30 seconds.

Figure 14 shows the transient response following ramp changes in the load. The steam flow to the turbine is changed at a rate of 10% per minute for a one-minute interval.

Throughout the one-minute interval, the control system changes the reactivity at the rate of -1.2×10^{-5} k/sec.

Figure 15 shows the pressure transient in the steam generator following a turbine trip-out. In the calculation, it is assumed that the reactor is scrammed 2 seconds after the trip-out and that a fraction of the steam flow to the turbine is bypassed to the turbine condenser. The results show that the peak in the pressure transient is a sensitive function of the fraction of steam that is bypassed. With no bypass, the pressure increases from 500 to 750 psi in 20 seconds. With 50% of the steam bypassed, the pressure increases to only 600 psi in 10-12 seconds.

TABLE I

Operating Chronology of HWCTR

July 1 - 13	Operated at 41 MW
13	Shut down - steam generator leak
14	Received fuel failure indications
14 - 26	Repaired leak in steam generator No. 1
17	Identified failed element
26	Attained criticality
27	Attained 30 MW
28	Attained 41 MW
29	Attained 42.5 MW
29 - 31	Operated at 42.5 MW
August 1	Attained 44 MW
1 - 7	Operated at 44 MW
7	Shut down - scheduled fuel inspections, annual tests
7 - 27	Inspected test and driver fuel, completed containment test, inspected and repaired steam generator No. 2
27	Attained criticality, 30 MW
28	Attained 40 MW
29	Attained 42.5 MW
29 - 31	Operated at 42.5-48.5 MW

TABLE II

Operating Summary of HWCTR

	July		August	
Time reactor critical, %	55.3		41.8	
Maximum power, MW	42.5		48.5	
Reactor exposure, MWD	Drivers	Test	Drivers	Test
For month	578	102	456	82
Total accumulated in Cycle H-2	1961	352	2417	434
Losses				
D_2O (100 mol %), lb	633		473	
% of inventory per year	10.9		~~12.0~~ 8%	
Deuterium, g	2986		2610	
Helium, scf	67,705		53,130	

TABLE III

Test Fuel Irradiation Data
July-August 1964[a]

Reactor power 42 MW (Cycle 2.3)
44 MW (Cycle 2.4)
48.5 MW (Cycle 2.5)
Coolant pressure 1200 psig

Coolant inlet temperature 185°C
Moderator outlet temperature 200°C
Coolant inlet temperature 230°C
(Liquid loop, position 38)

Position	Element Number[b]	Test Cycle[c]	Assembly Power[d], MW	Maximum Nominal Conditions: Specific Power[e], watts/g	Heat Flux, pcu/(hr)(ft²)	Outlet Temp., °C	Surface Temp., °C	Core-Clad Temp., °C	Core Temp., °C	∫kdθ, watts/cm	Maximum Exposure[e], watt-days/g: Attained	Goal
37	CANDU	2.3	1.09	29.3	143,000	213	216	239	-	29.3	6470	10,000
	TMT-1-3	2.5	1.16	60.3	464,000	211	259	402	519	-	305	20,000
38	SOT-6-2	All	0.56	45.8	259,000	244	266	320	-	28.0	2560	30,000
39	EMT-2(S/S)	2.3	0.70	95	470,000	197	247	368	440	-	-	-
	EMT-2(Zr)	2.4	0.88	120.0	595,000	198	261	414	504	-	3445	10,000
	SOT-8-2	2.5	1.03	68.3	334,000	199	241	351	-	31.9	345	30,000
40	SOT-1-4	2.3,2.4	0.63	75.6	338,000	193	235	333	-	26.7	-	-
	TMT-1-2	2.5	1.21	63.0	484,000	212	262	411	533	-	315	20,000
42	OT-1-2	2.3,2.4	0.76	67.1	312,000	194	231	325	-	24.8	12,020	30,000
	SOT-8-3	2.5	1.30	86.7	421,000	203	255	393	-	40.2	435	30,000
55	OT-1-7	2.3	0.62	60.5	280,000	195	231	315	-	22.3	-	-
	SOT-6-3	2.4,2.5	0.57	45.2	256,000	221	279	340	-	27.8	665	30,000
56	RMT-1-2	2.3,2.4	0.64	57.5	300,000	221	294	479	522	-	2735	10,000
	SOT-1-4	2.5	0.57	65.1	290,000	192	237	321	-	23.0	9925	30,000
57	SMT-1-2	2.3,2.4	0.59	40.1	310,000	206	296	367	430	-	4560	10,000
	OT-1-7	2.5	0.73	64.0	297,000	195	241	330	-	23.6	7830	30,000
58	SOT-1-2	All	0.59	66.0	296,000	192	230	316	-	23.4	15,210	30,000
59	SOT-9-2	2.5	0.84	65.3	370,000	229	297	384	-	40.0	330	20,000
60	SMT-1-3	2.3,2.4	0.46	42.3	328,000	202	304	378	445	-	4855	10,000
	OT-1-4	2.5	0.75	69.2	321,000	195	243	339	-	25.5	6405	30,000

(a) Data taken as follows: Cycle 2.3 - July 13; Cycle 2.4 - August 4; Cycle 2.5 - August 30; exposures as of August 31, 1964.
(b) Elements are identified in Table IV.
(c) Test cycles within the report period were: 2.3 July 1 to July 13
2.4 July 26 to August 8
2.5 August 25 to August 31
(d) "Flow-ΔT" power calculation; does not include moderator heating.
(e) These values are based on an assembly power of 1.09 times "Flow-ΔT" power to include moderator heating.

TABLE IV

Test Fuel Identification

Designation	Shape	OD	ID	Unit Length	Units	Fuel
CANDU	19-rod bundle	0.600" each	-	19-1/2"	5	Natural UO_2 sintered pellets in Zircaloy
SOT-1	Tube	2.06"	1.47"	14"	7	1.5% enriched UO_2 vibrated and swaged in Zircaloy
OT-1	Tube	2.06"	1.47"	10'	1	Same as SOT-1
SOT-6	Tube	2.54"	1.83"	14"	7	Natural UO_2 vibrated and swaged in Zircaloy
SOT-8	Tube	3.67"	2.99"	14"	7	1.2% enriched UO_2 vibrated and swaged in Zircaloy
SOT-9	Tube	2.54"	1.83"	14"	7	1.2% enriched UO_2 vibrated and swaged in Zircaloy
TMT-1	Tube	2.55"	1.85"	10'	1	1.4% ^{235}U in thorium core in Zircaloy
EMT-2	Tube	2.06"	1.70"	37"	1	3% enriched uranium alloyed with 1.5% Mo in Zircaloy
SMT-1-2	Tube	1.70"	1.24"	11-1/4"	10	Natural uranium alloyed with Fe, Al in Zircaloy
SMT-1-3	Tube	1.70"	1.24"	11-1/4"	15	Natural uranium alloyed with Fe, Al, Si, in Zircaloy
RMT-1-2	Tube	2.07"	1.57"	10'	1	Unalloyed natural uranium in 60-mil Zircaloy cladding

TABLE V

Dimensional Changes of HWCTR Drivers[a]

Fuel Tube No. 1	First Exposure Period (39 days)[b]	Second Exposure Period (38 days)[b]	Total (77 days)[b]
Maximum metal temp., °C	535-540	560-575	-
Maximum burnup, atom %	0.336	0.437	0.773
OD change, %[c]	-0.2	+0.2	0
ID change, %[c]	+0.1	-0.3	-0.2
Volume change, %[c]	-1.6	+2.6	+1.0
Fuel Tube No. 18			
Maximum metal temp., °C	535-540	575-585	-
Maximum burnup, atom %	0.336	0.452	0.788
OD change, %[c]	-0.2	+0.1	-0.1
ID change, %[c]	-0.05	-0.2	-0.2
Volume change, %[c]	-0.8	+1.0	+0.2

(a) Driver fuel cores are U-Zr alloy (9.3 wt % U, fully enriched); the tubes were fabricated by coextrusion in Zircaloy-2 sheaths. The clad tubes are 1.96-in. ID, 2.30-in. OD, and 10-ft length.
(b) Equivalent days of full-power operation.
(c) At point of maximum burnup.

TABLE VI

Control Rod Designs for D_2O-Cooled Reactor

Material: stainless steel

Control Rod Type	OD	ID	Geometry	$1/\delta$[a], cm
1	0.6 in.	-	Solid rod	0.2341
2	0.8 in.	-	Solid rod	0.3532
3	1.0 in.	-	Solid rod	0.4674
4	1.0 in.	0.8 in.	Tube	0.2444
5	1.28 in.	1.0 in.	Tube	0.3776
6	1.56 in.	1.2 in.	Tube	0.5070
7	Rod 1 inside Rod 4		Rod and tube	0.3902
8	Rod 2 inside Rod 5		Rod and tube	0.5506
9	Rod 3 inside Rod 6		Rod and tube	0.6887

(a) See Section IIA of text for definition of δ.
(b) Fuel design is shown in Figure 11.

TABLE VII

Bend Tests on Half-Ring Sections from Irradiated Driver Housing No. 19

Material: Low-nickel Zircaloy-2

Position of Specimen in Housing	Relative Neutron Flux	Typical Coolant Temp., °C	Force Required, lb	Cracks	Corrosion: ZrO_2 Thickness, mil	Corrosion: Calculated Weight Gain, md/dm²	Metallographic Estimate of Hydrogen Content, ppm
Top	0.27	190	40-48	No	0.17-0.23	63-86	<50
Middle	0.97	200	53-59	No	~0.18	67	<50
Bottom	0.34	205	56-64	No	0.10-0.18	37-67	<50
Unirradiated	0.00		30-40	No			~10
Corrosion expected in an autoclave in 6000 hr at 200°C					0.03	11	

TABLE VIII

Design Parameters of 1000-MWe Liquid D_2O-Cooled Reactor

Fuel Design	
Fuel geometry	Tubes
Fuel material	UO_2
Number of fuel tubes	3
Cladding material	Zircaloy-2 or -4
Pressure tube material	Zr - 2.5% Nb
Calandria tube material	Zircaloy-2 or -4
Lattice pitch, in.	10.5
System pressure, psia at outlet header	1700
Design pressure, psia	2000
Design temperature, °C	321
Cladding thickness, mils	25
Weight of fuel, lb/ft UO_2	20
Inlet temperature, °C	264
Max. outlet temperature, °C	315
Min. outlet temperature, °C	290
Moderator outlet temperature, °C	90
Outer coolant channel thickness, in.	0.180
Fuel length, in.	180
Fuel density, UO_2, % theoretical	92
^{235}U content, %	1.185
H_2O in moderator, %	0.3
Calandria tube thickness, mils	60
Insulating annulus thickness, mils	120
Power of avg. flat zone assembly, MWt	7.6
Max. assembly power, MWt	9.9
Max. subchannel velocity, ft/sec	50
Flow, gpm at 264°C	750
Friction loss, psi	50
Max. surface temperature, °C	330 (local boiling)
Max. $\int k d\theta$, inner and intermediate tubes, watts/cm	42
Max. $\int k d\theta$, outer tube, watts/cm	32
Max. heat flux, pcu/(hr)(ft^2)	520,000
Calandria tube (Zircaloy-2)	
OD, in.	4.93
ID, in.	4.81
Pressure tube (Zr - 2.5% Nb)	
OD, in.	4.57
ID, in.	4.12
Housing tube	
OD, in.	4.00
ID, in.	3.94
Fuel tubes - Clad diameters	
No. 1 OD, in.	3.58
ID, in.	3.09
No. 2 OD, in.	2.49
ID, in.	1.89
No. 3 OD, in.	1.24
ID, in.	0.61
Core Design	
Thermal power, MW	3520
Moderator power, MW	140
Number of fuel positions	516
Number of control and safety positions	183
Min. reactivity in control, %	1.0

Core Design (Continued)	
Core radius, in.	135
Flat zone radius, in.	104
Radial reflector, in.	16
Core length, ft.	15
Axial reflector, in.	18
Inlet temperature, °C	264
Outlet temperature, °C	300
Total coolant flow, gpm at 264°C	350,000
No. of coolant loops	6
Fuel inventory, TU	62
Avg. specific power, MW/TU	59
Fuel exposure in B.Z., MWD/TU (on-power fueling)	15,000
Fuel exposure in F.Z., MWD/TU (on-power fueling)	22,000
Avg. exposure, MWD/TU	19,000
Shield Design (based on shielding requirements)	
Shield Thickness	
Radial thermal, in.	12
Top thermal, in.	21
Bottom thermal, in.	21
Radial biological, in.	114
Shield Heat Load, Btu/hr	
Radial thermal	250,000
Top thermal	260,000
Bottom thermal	260,000
Steam Generator Design	
Input power to steam generators, MW	2980
Over-all U, pcu/(hr)(ft^2)(°C)	800
Mean ΔT, °C	29
Heat transfer area, ft^2	244,000
Pressure on steam side, psia	630
Steam temperature, °C	254
Economizer Design	
Input power to economizers, MW	590
Over-all U, pcu/(hr)(ft^2)(°C)	400
Mean ΔT, °C	40
Heat transfer area, ft^2	70,000
Turbine Design	
No. of feedwater heaters	4
Feedwater temperature, °F	360
Throttle pressure, psia	600
Gross turbine efficiency, %	30.4
Gross electrical output, MW	1085
Power used by auxiliaries, MW	85
Net electrical power, MW	1000
Reactor fission power, MW	3660
Net system efficiency, %	27.3
Pressure Drops, ft of coolant at 264°C	
Pigtails	130
Pressure tube extensions	130
Coolant headers	10
Primary coolant piping	160
Steam generator	40
Fuel assembly	140
TOTAL	610

TABLE IX

Input Data and Steady-State Values for Kinetics Study of 1000-MWe Reactor

Input Constants	Steady-State Values
H_1 = 20 MW-sec/°C	T_1^o = 1000°C
H_2 = 40 MW-sec/°C	T_2^o = 304.2°C
H_3 = 500 MW-sec/°C	T_3^o = 304.2°C
H_4 = 2500 MW-sec/°C	T_4^o = 264.2°C
H_5 = 700 MW-sec/°C	T_5^o = 264.2°C
U_1 = 5.0838 MW/°C	C_1^o = 1.0
U_2 = 160.8 MW/°C	C_2^o = 1.0
F_1 = 91.0 MW/°C	C_3^o = 1.0
F_2 = 9.917 MW/°C	C_4^o = 1.0
m = 0.040 lb/mol	n_s^o = 0.4954 x 10^6 mol
h = 0.80 MW-sec/lb	P_s^o = 501.6 psia
R = 0.0426 psi-ft^3/°K-mol	P_o = 3640 MW
V_s = 22,800 ft^3	
G_1 = 4000 lbs/sec	
λ_1 = 0.02484	
λ_2 = 0.1993	
λ_3 = 1.384	
λ_4 = 0.2360 x 10^{-3}	
β_1 = 0.001826	
β_2 = 0.004442	
β_3 = 0.001121	
β_4 = 0.0000908	
α_1 = 1 x 10^{-5}/°C	
α_2 = 0	
T_8 = 197.0°C	

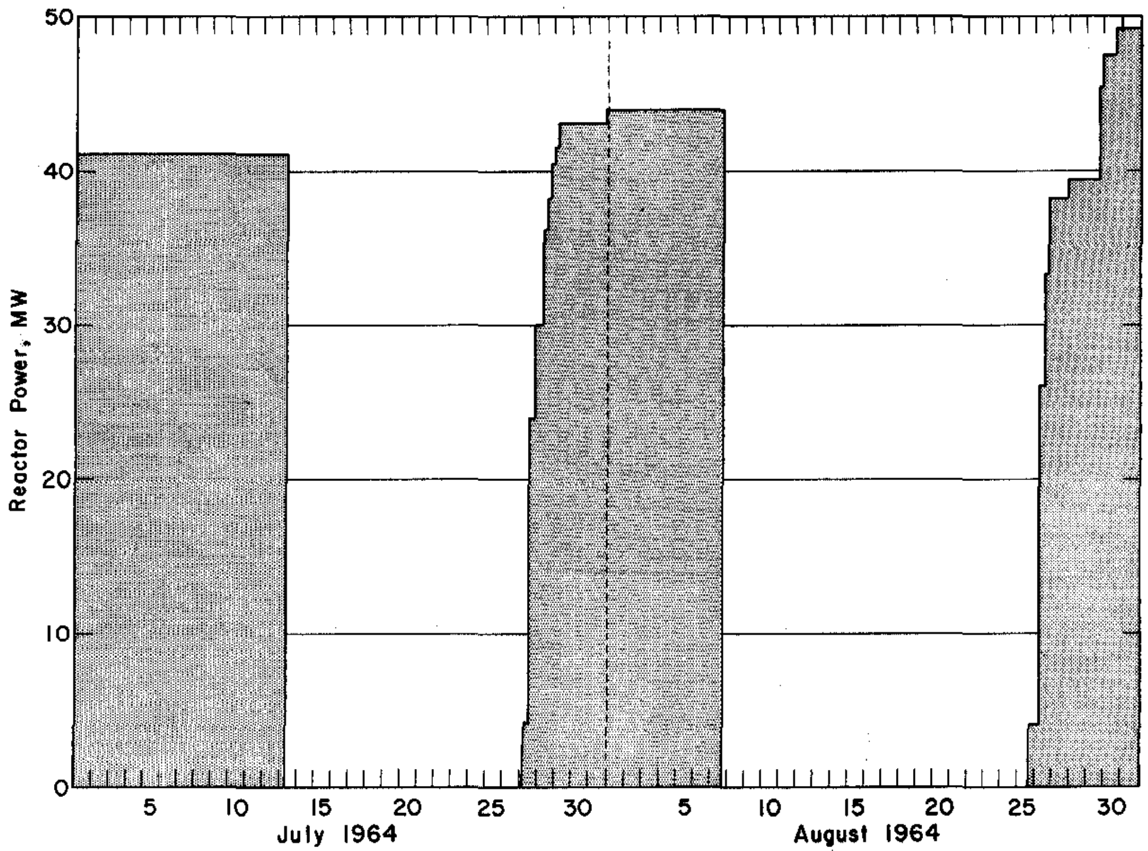

FIG. 1 OPERATING POWER OF HWCTR

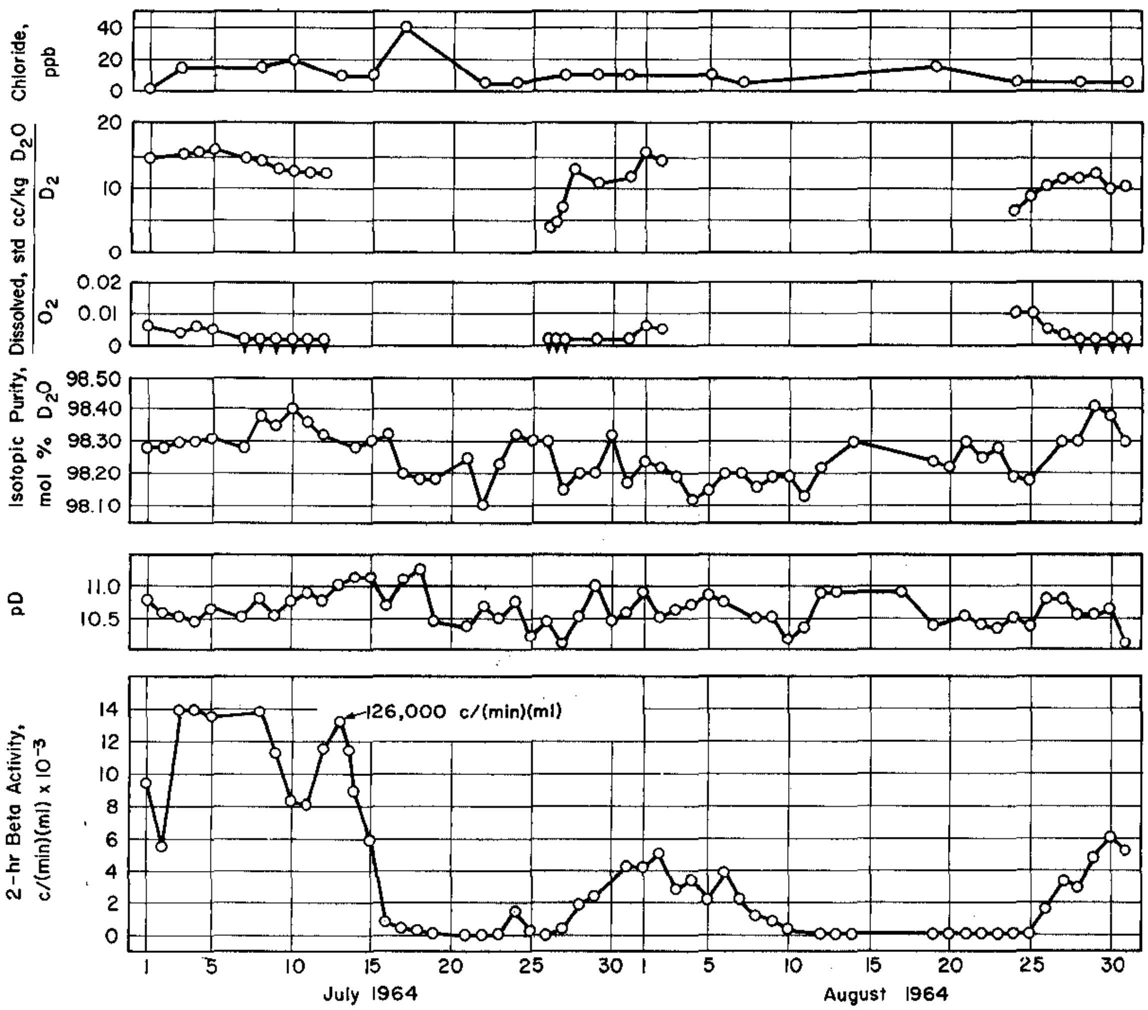

FIG. 2 HEAVY WATER QUALITY IN HWCTR

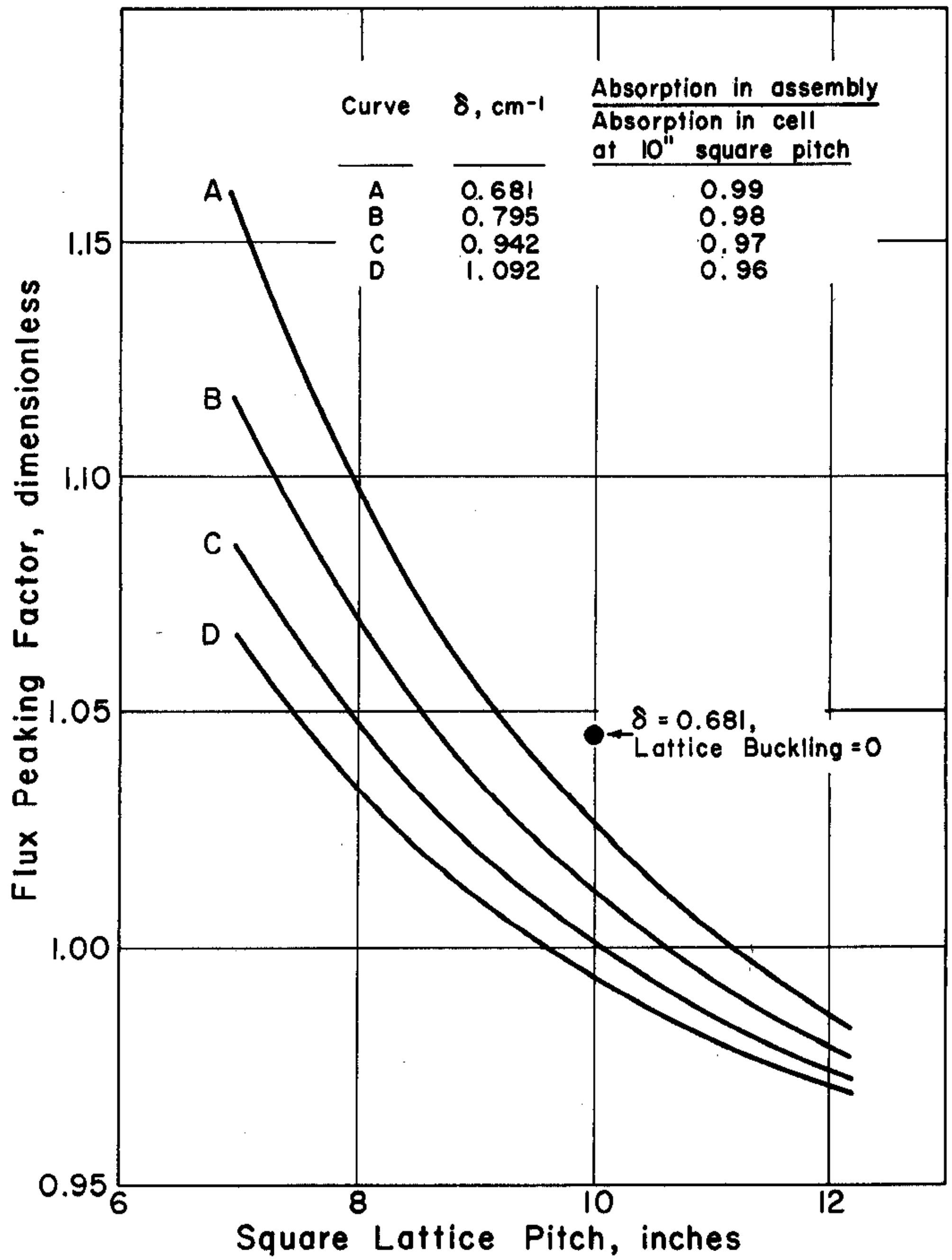

FIG. 3 FLUX PEAKING IN FUEL ADJACENT TO EMPTY FUEL POSITION

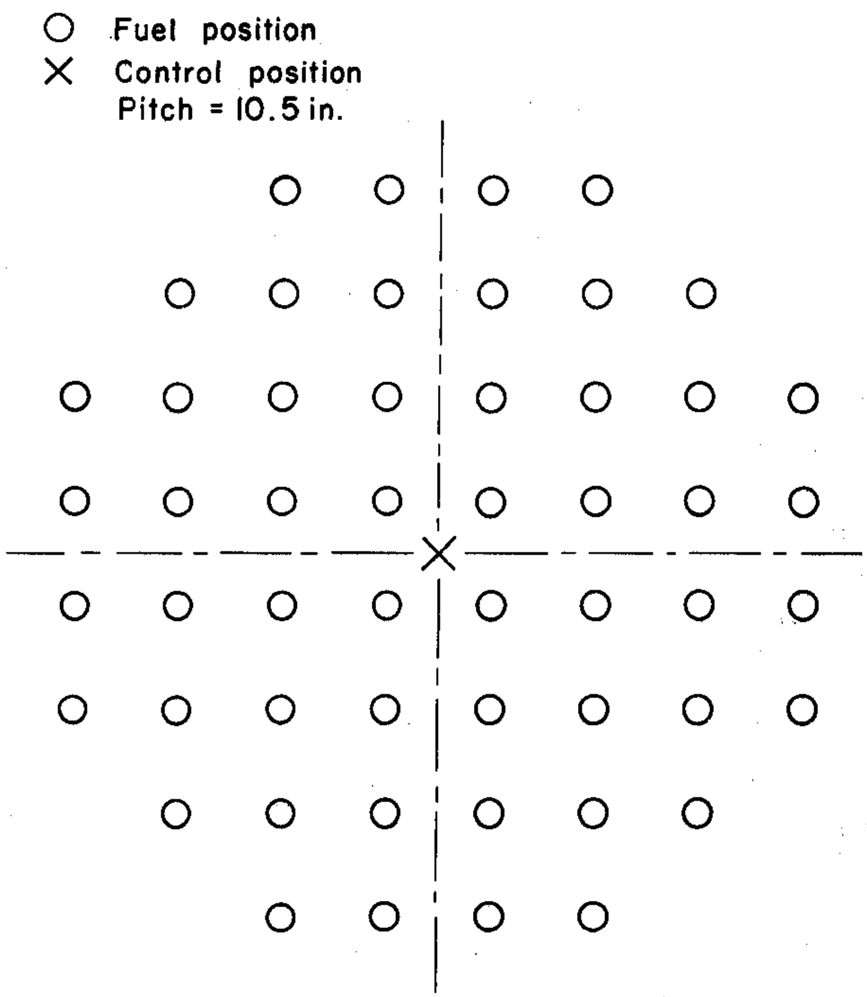

FIG. 4 SMALL REFERENCE LATTICE FOR CONTROL ROD CALCULATIONS

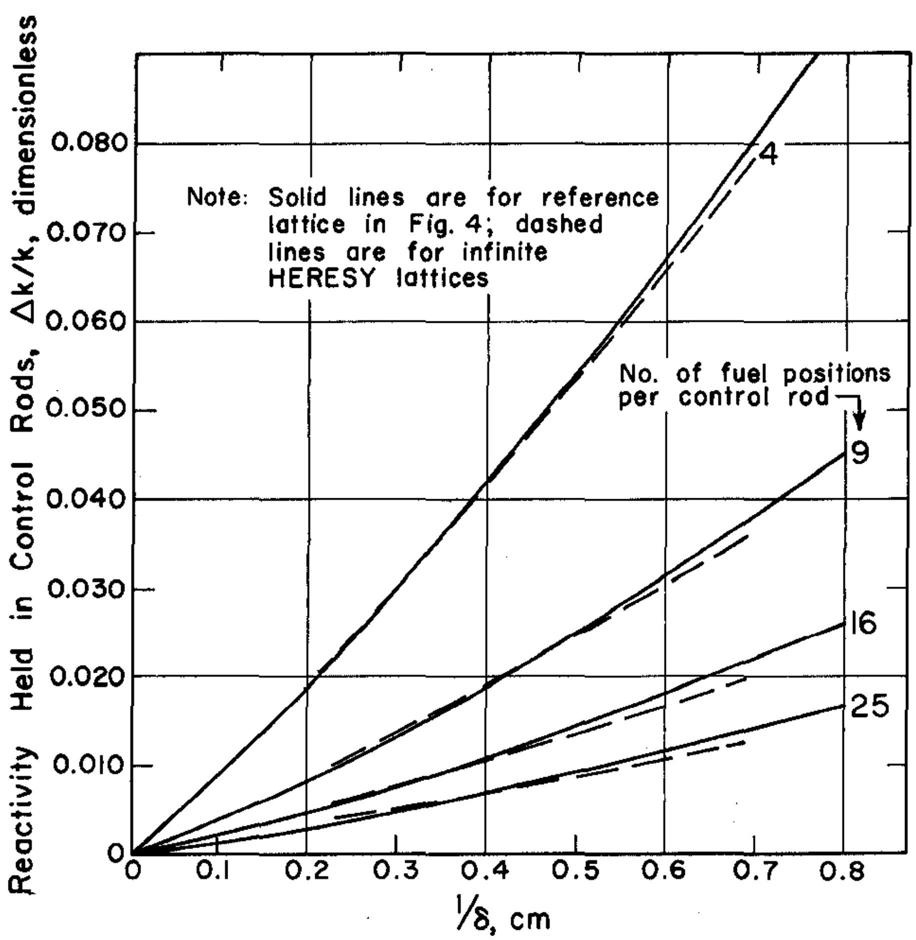

FIG. 5 REACTIVITY HELD IN CONTROL RODS

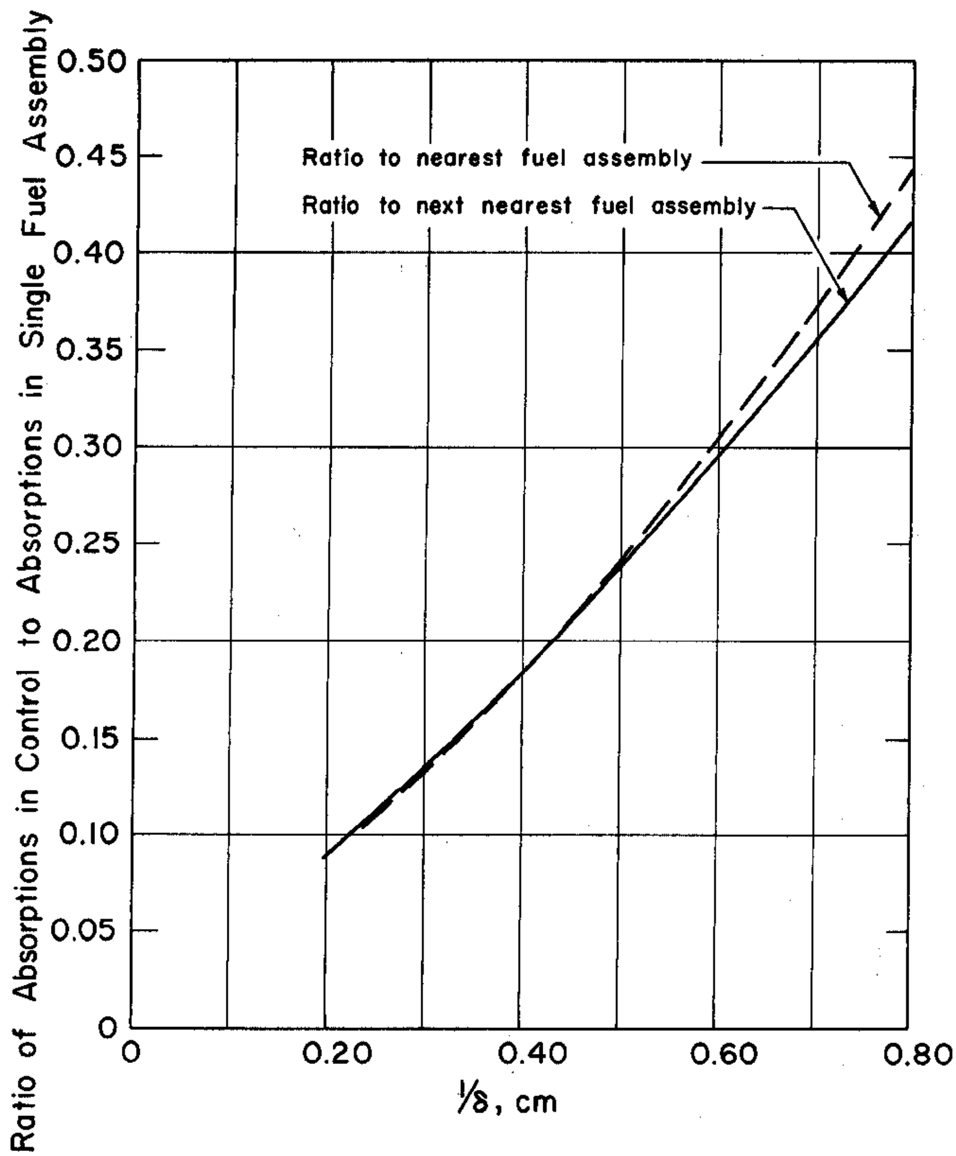

FIG. 6 NEUTRON ABSORPTION RATIOS FOR SINGLE CONTROL ROD IN SMALL FINITE LATTICE

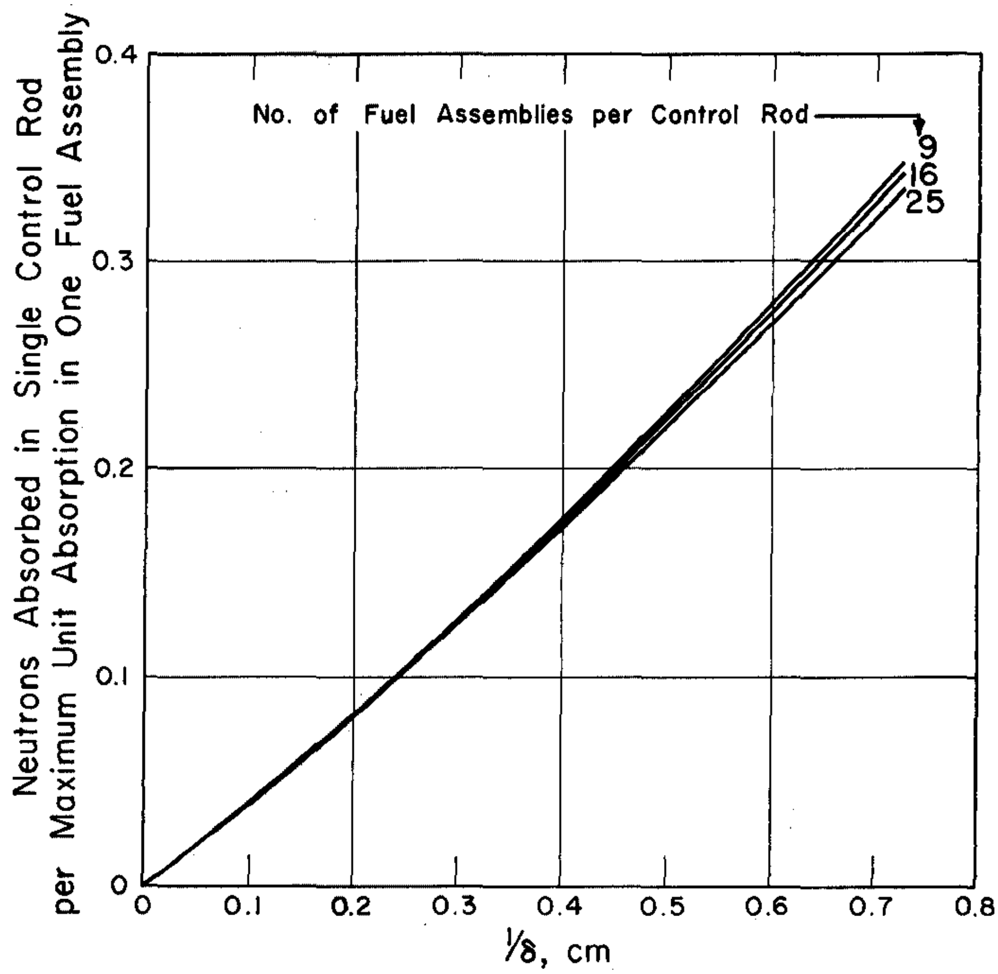

FIG. 7 NEUTRON ABSORPTION RATIOS

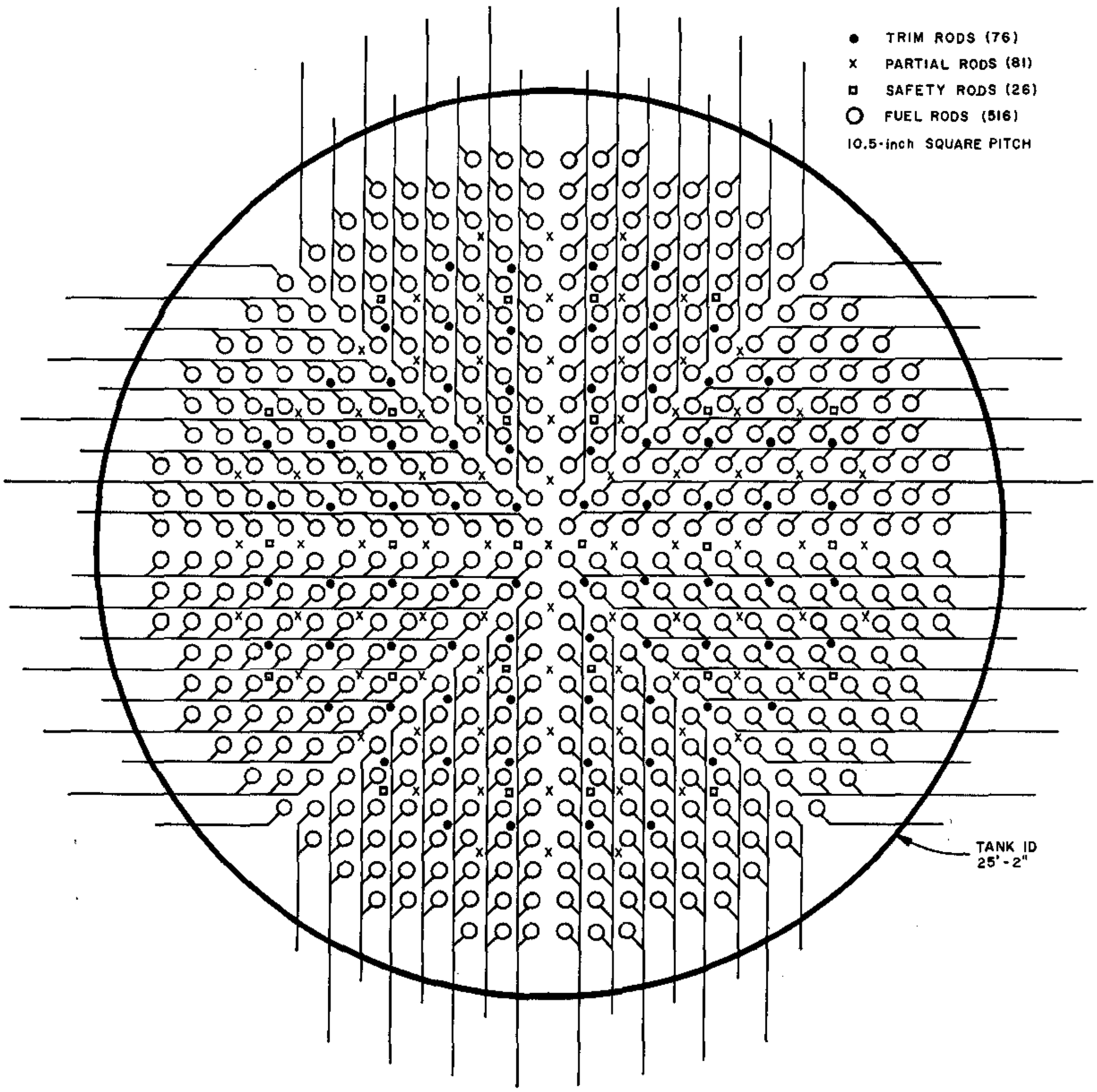

FIG. 8 RECOMMENDED LATTICE FOR DESIGN STUDY OF 1000-MWe D_2O-COOLED REACTOR

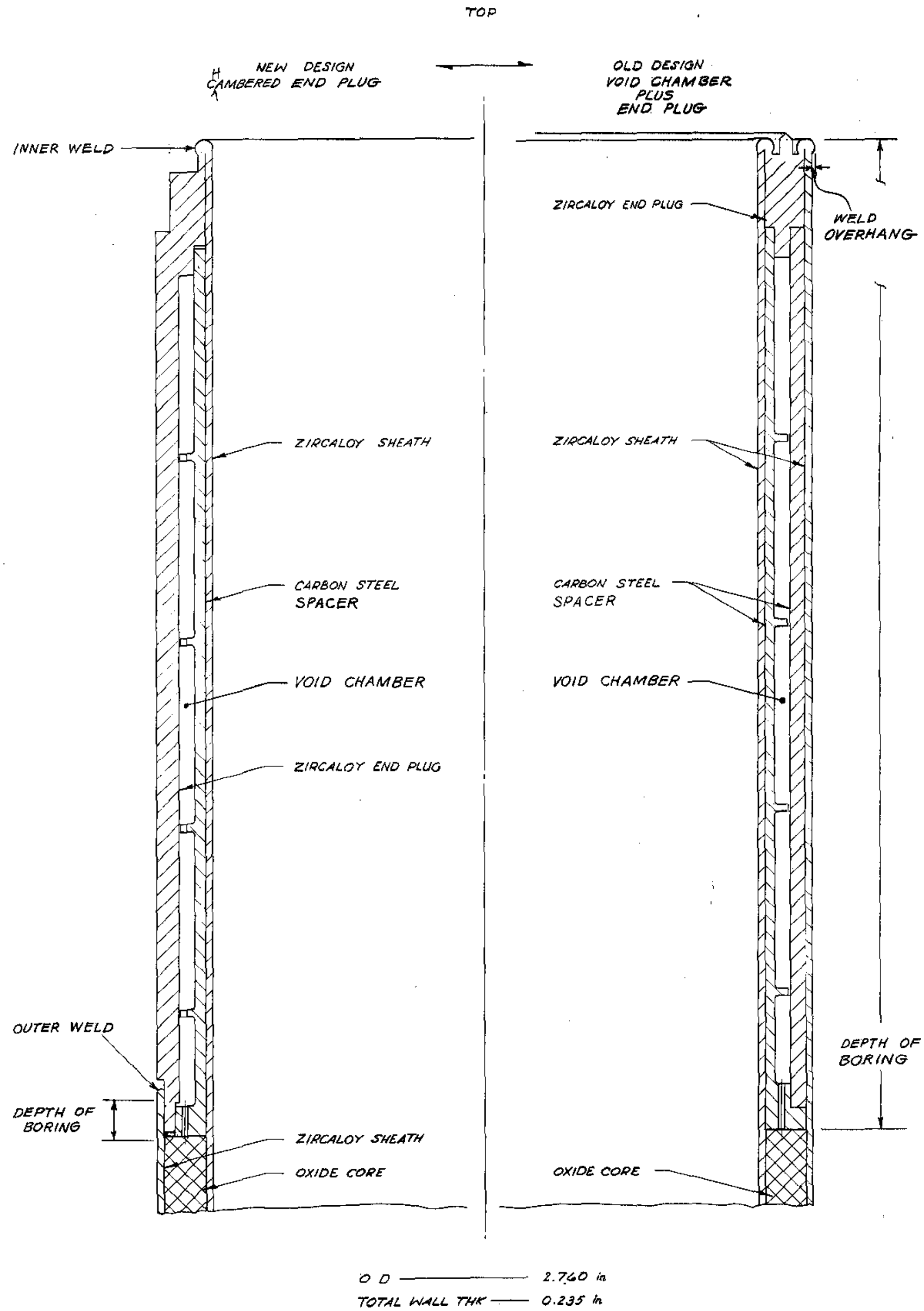

FIG. 9 COMPARISON OF END PLUG DESIGNS FOR UO_2 FUEL TUBES

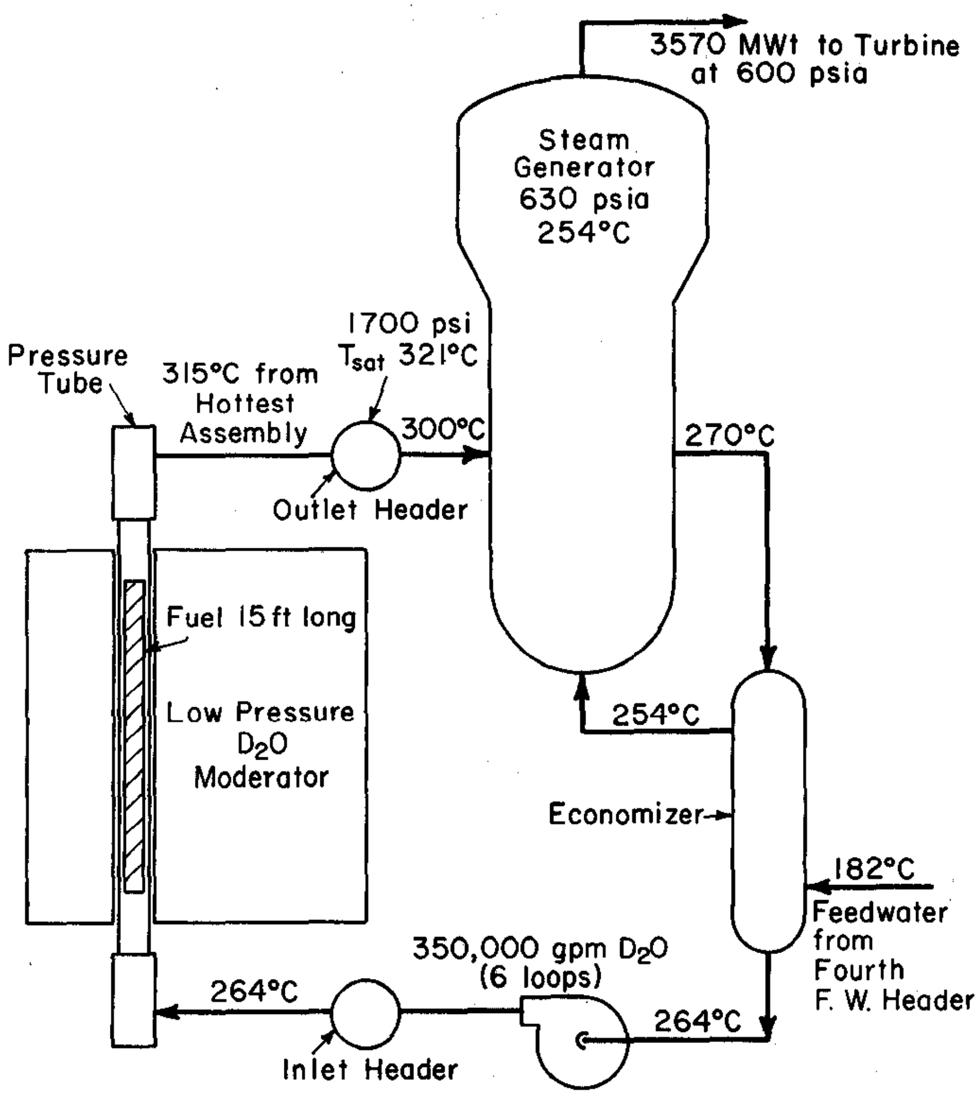

FIG. 10 FLOWSHEET FOR 1000-MWe D_2O-COOLED REACTOR

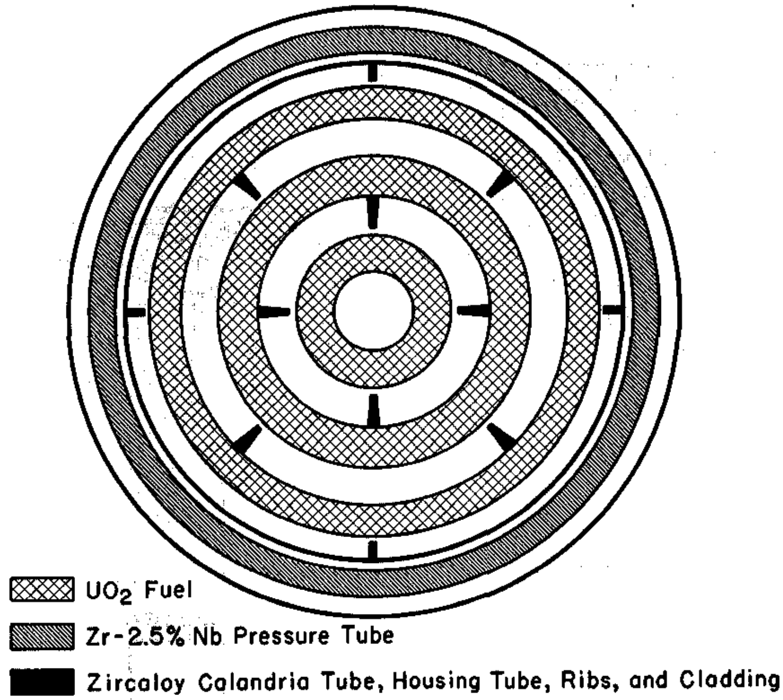

FIG. 11 FUEL ASSEMBLY FOR D_2O-COOLED-AND-MODERATED REACTOR

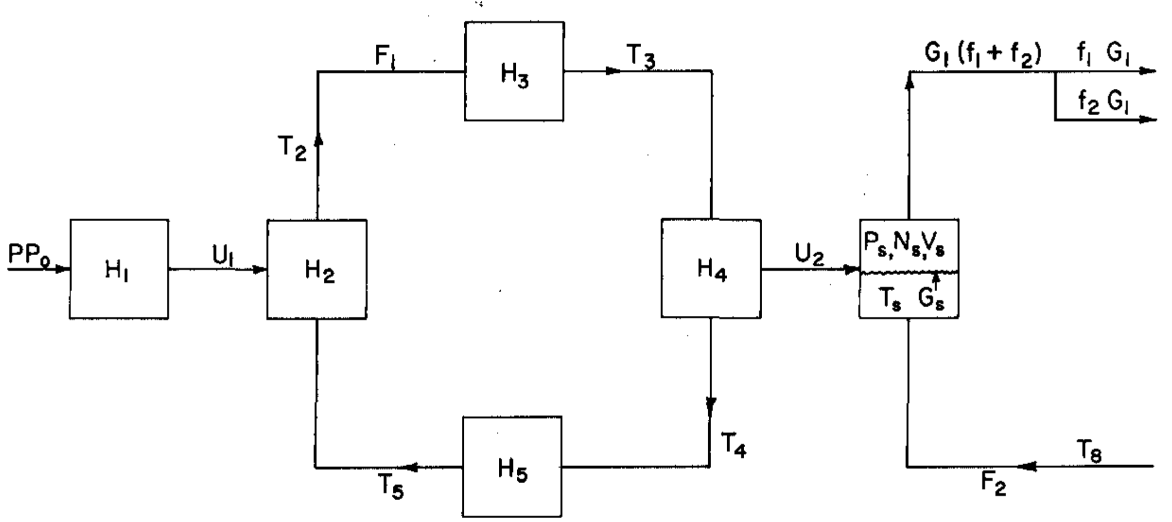

FIG. 12 MATHEMATICAL MODEL FOR KINETICS STUDIES OF 1000-MWe D_2O-COOLED REACTOR

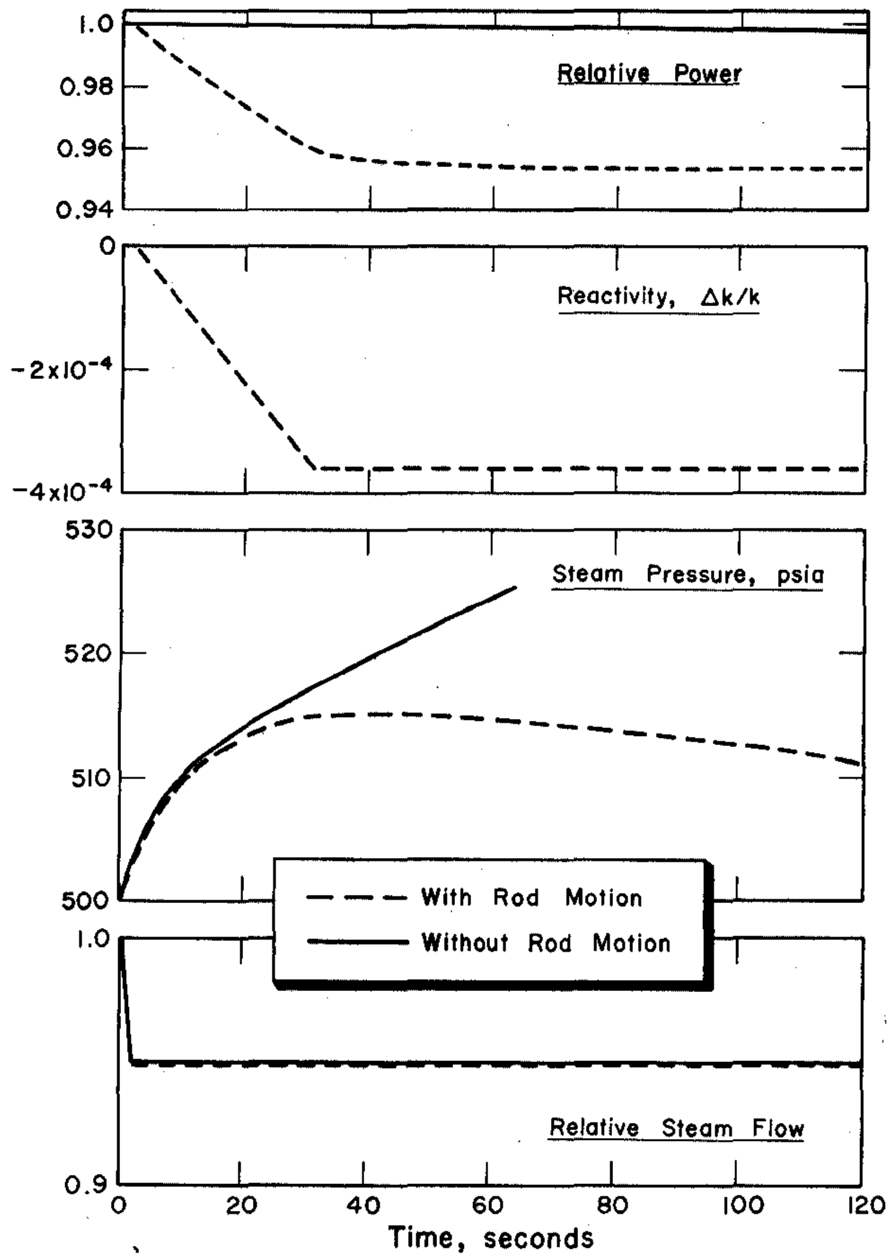

FIG. 13 RESPONSE OF 1000-MWe D_2O-COOLED REACTOR TO 5% STEP DECREASE IN TURBINE LOAD

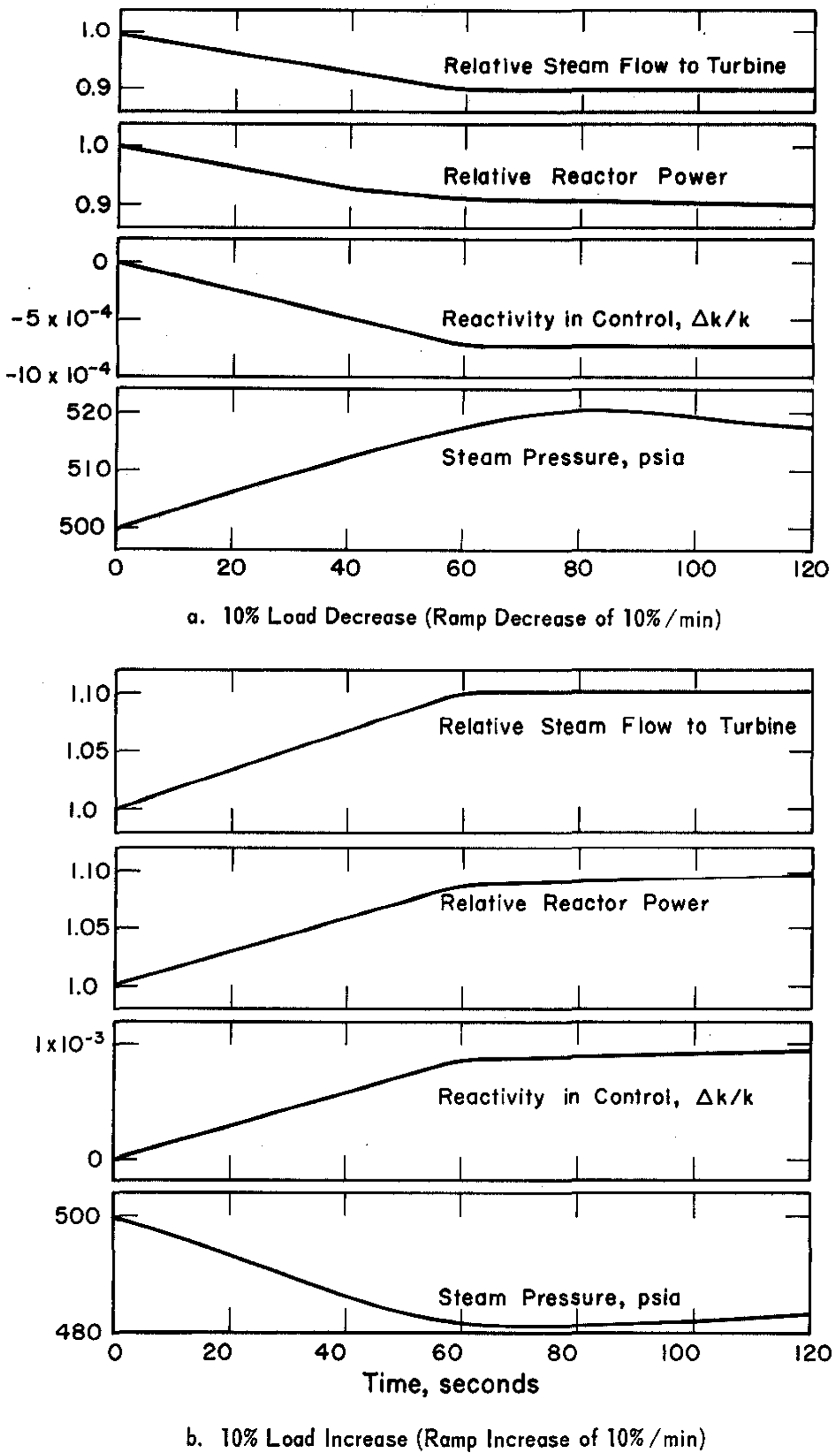

FIG. 14 RESPONSE OF 1000-MWe D_2O-COOLED REACTOR TO RAMP CHANGES IN TURBINE LOAD

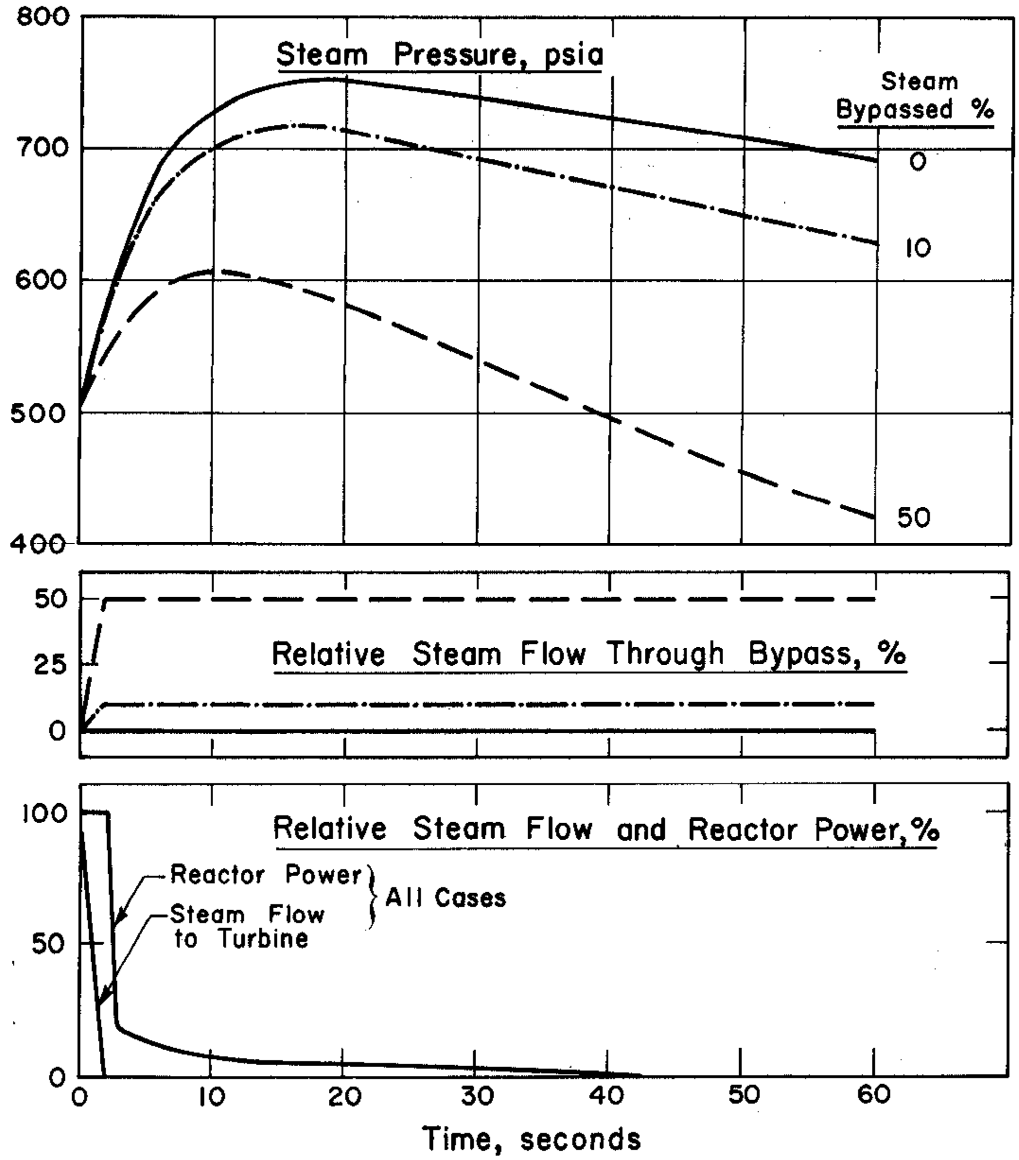

FIG. 15 STEAM PRESSURE TRANSIENT FOLLOWING A TURBINE TRIP AND REACTOR SCRAM

BIBLIOGRAPHY

1. Klahr, C. N., et al. Heterogeneous Reactor Calculation Method. Quarterly Progress Report No. 6, Technical Research Group 129, TRG, Inc., Syosset, N. Y. USAEC Report NYO-2678 (1960).

2. Babcock, D. F., et al. An Evaluation of Heavy-Water-Moderated Power Reactors - A Status Report as of March 1963. E. I. du Pont de Nemours & Co., Savannah River Laboratory, Aiken, S. C. USAEC Report DP-830 (1963).

3. Pressurized Water Reactor (PWR) Project - Technical Progress Report for the Period January 24, 1964 to April 23, 1964. Westinghouse Electric Corp., Bettis Atomic Power Lab., Pittsburgh, Pa. USAEC Report WAPD-MRP-108 (1964).

4. Previous progress reports in this series are:

DP-232	DP-395	DP-485	DP-575	DP-665	DP-755	DP-845
DP-245	DP-405	DP-495	DP-585	DP-675	DP-765	DP-855
DP-265	DP-415	DP-505	DP-595	DP-685	DP-775	DP-865
DP-285	DP-425	DP-515	DP-605	DP-695	DP-785	DP-875
DP-295	DP-435	DP-525	DP-615	DP-705	DP-795	DP-885
DP-315	DP-445	DP-535	DP-625	DP-715	DP-805	DP-895
DP-345	DP-455	DP-545	DP-635	DP-725	DP-815	DP-905
DP-375	DP-465	DP-555	DP-645	DP-735	DP-825	DP-915
DP-385	DP-475	DP-565	DP-655	DP-745	DP-835	